8×8 Near-Field Focused Circularly Polarized Cylindrical DRA Array for RFID Applications

Saber H. Zainud-Deen, Hend A. Malhat, and Kamal H. Awadalla

Department of Electronics and Electrical Communications Engineering
Faculty of Electronic Engineering, Menoufiya University, Egypt
anssaber@yahoo.com, er_honida@yahoo.com

Abstract **─** The design of an 8×8 near-field focused circularly polarized dielectric resonator antenna (DRA) array for fixed RFID reader applications at 5.8 GHz is presented. The proposed antenna array consists of 64-element of cylindrical dielectric resonator antennas (CDRA) with two orthogonal feeding probes located inside the CDRA element. A single element CDRA with supporting arms is used as a building block of the array provided good impedance matching and circular polarization at 5.8 GHz. The perforation technique is used for the supporting arms to reduce the manufacturing complexities in the CDRA mounting over the ground plane. The sequential feeding technique is applied to improve the gain and circular polarization bandwidth of the single element and the array. The characteristics of the near-field focused array are introduced compared to that of the uniformly phased array. The finite integral technique and the finite element method are used to compute the array performance.

Index Terms **─** CDRA, fixed reader antenna, RFID, sequential feeding.

I. INTRODUCTION

RFID systems have been applied in many applications for their advantages over other automatic identification systems [1]. Practically, the RFID reader has a read zone that can sometimes be difficult to control due to multipath effects or reflections of the RF signal. Problems that may arise with conventional RFID readers include:1) the reader may detect tags that are not in the reader coverage area, and 2) the tags may be located adjacent to the reader antenna thus blocking its field. Spatial isolation of an RFID tag may be difficult if the interrogation range of the RFID readers is not easily controlled or adjusted to a lower power setting. This can lead to errors in customer purchases or errors in verification that an item is in a specific physical location (e.g., baggage on a specific cart) [2, 3]. The RFID reader antenna is an important component in RFID systems and it has been designed with circularly polarized (CP) operation. CP for the reader antenna in transmission is preferred because the tag antenna (which is linearly polarized) will receive enough power from the transmitter irrespective of its orientation. A CP antenna with a low profile, small size, lightweight, high gain, and high front-to-back ratio is required in a portable RFID reader [4-6]. The other type of RFID reader is the fixed reader. Generally, fixed-reader antennas are complex microstrip patch arrays with high gain, and a relatively narrow beam and low side lobe level [7-9].

Using antenna arrays for a fixed RFID reader will result in long read range. The far-field region is determined according to the dimensions of the array (L×L) and the operating frequency by ($2L^2/\lambda$). In some applications, tags may be located in the near-field region of the fixed reader antenna array not in their far-field region as is usually the case in a standard communication system. Therefore, a reader antenna array exhibiting a near-field (NF) focused radiation, which is able to maximize the field amplitude in a size-limited spot within the antenna near-field region, while not affecting the field strength far from the antenna (far-field region), is needed. Recently, NF-focusing has attracted major interest due to its potential applications in near-field sensing and imaging microscopy [10-11]. NF- focusing is used in RFID to increase the field incident on the tags at allowed effective isotropic radiated power (EIRP)

Submitted On: Aug 6, 2011
Accepted On: Oct 23, 2011

[12-14]. In [15], a circular half-wavelength dipole array is used to study the effect of changing the focusing distance on the power in the Fresnel region. In this paper, an 8×8 NF-focused cylindrical DRA phased array with supporting arms for fixed RFID reader at 5.8 GHz is proposed. The NF-focused CDRA array is designed to maximize the radiated power density in a limited size spot in the near field of the RFID reader. The performance parameters of the NF-focused array are compared with that of uniform phased array. The array consists of 64 sequentially fed CDRA elements with two supporting arms mounted on a square ground plane. Each CDRA element is fed via two orthogonal probes located at two orthogonal points from the CDRA center. The finite integration technique (FIT) [16] is used to optimize and analyze the antenna array performance parameters such as reflection coefficient, radiation pattern and antenna gain. The finite element method (FEM) [17] is used to validate the results. The novelty of this work is the using of the CDRA elements in the phased array for wide bandwidth, no metallic loss (high radiation efficiency), and high gain (wide coverage area for RFID reader). The paper is organized as follows. In Section II, numerical results for a circularly polarized CDRA with supporting arms as a building block for the RFID reader antenna array are investigated. Near field focused CDRA array for fixed RFID reader consists of 64 CDRA elements is designed at 5.8 GHz. Section III concludes the results.

III. NUMERICAL RESULTS

Figure 1 shows the geometry of a single cylindrical dielectric resonator antenna with two feed probes excitation. The CDRA with dielectric constant ε_r of 10.2 is used [18]. It has a radius '*a*' of 5.9 mm and a height 'H_d' of 8.3mm. The CDRA is designed to operate around 5.8 GHz. Two coaxial probes are located off the center by distance d_f of 5.1 mm. Each probe has radius of 0.25 mm and height h_f of 3.9 mm. The two probes are parallel and located at similar positions on two orthogonal diameters and the feeding is arranged such that the two probes have a phase difference of 90^o. Because of the fabrication complexity of CDRA over ground plane, four supporting arms having rectangular shape are connected with the CDRA. In [19], perforated structure was proposed to overcome the mounting problems of the CDRA over the ground plane and save more manual effort in the alignment of the CDRA with the feeding structure especially for arrays. The technique of perforating a dielectric sheet eliminates the need to position and bond individual CDRA elements in the array. Perforations create different effective dielectric permittivity and make the fabrication of CDRA arrays feasible. The perforations result in lowering the effective dielectric constant for the region between the CDRA elements. The CDRA element is made from one piece of dielectric material; with a perforated bonding dielectric rods and completely eliminating all the rest of the dielectric material. The dielectric rods have low dielectric constant and thin enough to avoid guiding waves around the design frequency of the element itself. The effective dielectric constant, ε_{reff}, of the perforated material can be calculated from [19]

$$\varepsilon_{r\,eff} = \varepsilon_r(1-\alpha)+\alpha\,,$$

$$and \quad \alpha = \frac{\pi R_p^2}{2\left(\sqrt{3}/4\right)\; S_p^2} \tag{1}$$

where R_p is the radius of the air holes, and S_p is the center to center separation distance of the holes. The holes forming the perforation are only one line centered along the axis of the ribbon forming the supporting arm. Thus, the supporting arms are used to reduce the fabrication complexity while keeping the same radiation characteristic as arm free element [19, 20].

The dimensions of the supporting arms are width W_p= 4 mm and thickness H_p=1 mm. The supporting arms are perforated by incorporating air holes in the arms. The air holes have equal radii, R_p=1.2 mm and center to center separation S_p=3R_p. The CDRA elements with supporting arms are mounted on square ground plane with edge length 'G' of 35.15 mm. Figure 2 shows the simulated reflection, S_{11}, at the two ports of the feeding pins of the single CDRA element with perforated supporting arms against the frequency. The two ports produced the same performance due to their position similarity. Good impedance matching is obtained with impedance bandwidth extending from 5.62 GHz to 6.12 GHz for S_{11} < -10 dB.

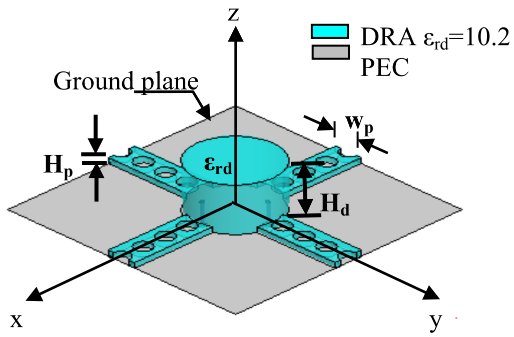

a. 3-D view

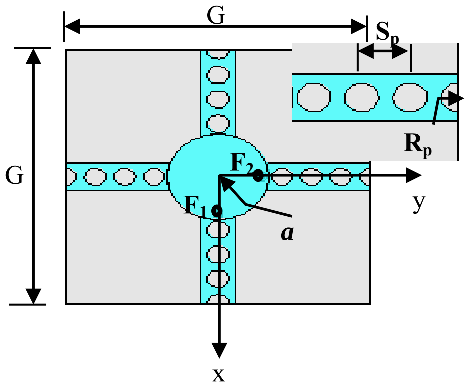

b. Top view

Fig. 1. The geometry of circularly polarized CDRA with supporting arms.

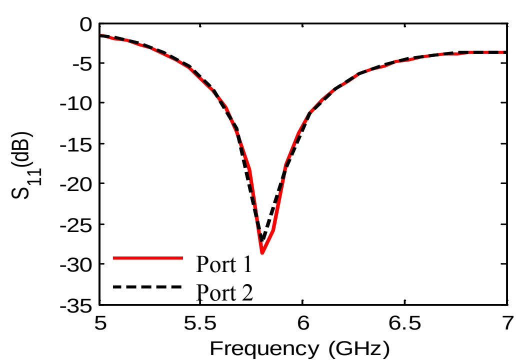

a. Reflection coefficient

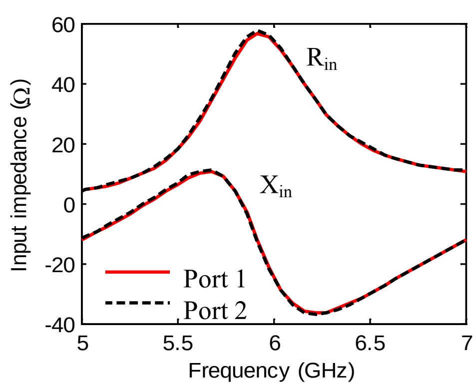

b. The input impedance

Fig. 2. The power reflection coefficient and input impedance versus frequency of the CDRA with supporting arms.

The simulated radiation pattern components, left hand polarization, E_L, and right hand polarization, E_R, of the single CDRA element at 5.8 GHz in x-z plane and y-z plane are shown in Fig. 3. Asymmetrical radiation pattern is obtained with high cross-polarization level due to the coupling effect between the excitation orthogonal probes, as well as the asymmetrical positioning of the feeds with respect to the two planes. Good agreement is obtained between the results calculated by FEM and FIT techniques.

The main polarization (E_L) is within -10 dB level in a beam of about 100° width centered at the 0° direction. The cross polarization (E_R) level is more than -10 dB relative to the main polarization (E_L) within the circular polarization beam (100°). These results indicate good performance of this dielectric resonator antenna for RFID reader application.

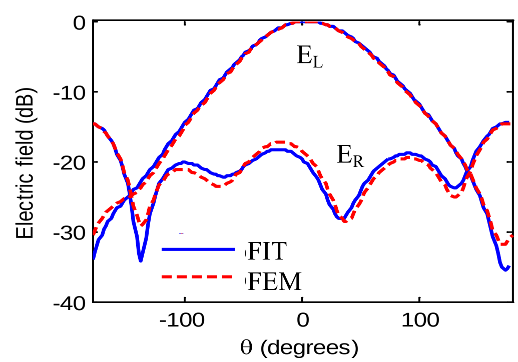

a. x-z plane

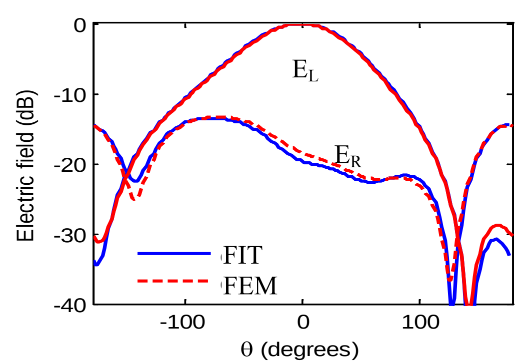

b. y-z plane

Fig. 3. The simulated radiation pattern components of the single element at 5.8 GHz.

The axial ratio at the normal axis, $\varphi = \theta = 0^o$, versus frequency is shown in Fig. 4a. The antenna provides circular polarization with minimum value of 1.9 dB at 5.8 GHz with a relatively wide axial ratio bandwidth (AR< 3dB) of the order of 40.74%. The antenna gain at the normal axis over the operating band is shown in Fig. 4b. The gain at the normal axis is 7.15 dB at 5.8 GHz and nearly constant within 0.5 dB over the RFID frequency band (5.65- 5.95 GHz).

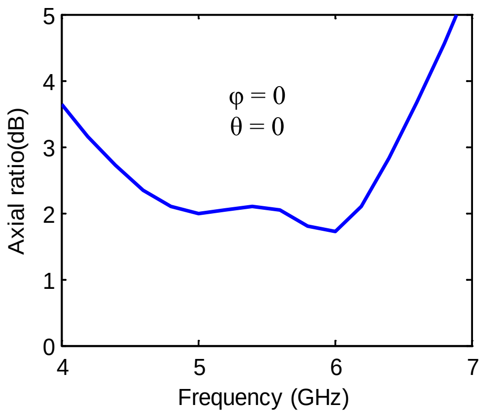

a. Axial ratio

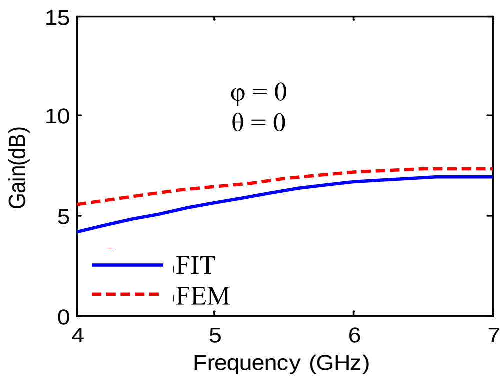

b. Gain

Fig. 4. The simulated axial ratio and antenna gain versus frequency of the single element CDRA with supporting arms.

An 8×8 RFID reader antenna array with supporting arms is shown in Fig. 5. The area of the array is L×L= 28.13 × 28.13 cm^2 (5.44 λ×5.44 λ where λ is the free-space wavelength at 5.8 GHz). The distance G between the elements is 35.16 mm (0.68λ) to reduce the mutual coupling between the elements. The sequential feeding technique is applied to the CDRA elements in order to improve the circular polarization bandwidth (axial ratio bandwidth) and gain of the antenna array [21]. For each sub-array forming (2×2) elements, the elements in one diagonal are 90^o out of phase and rotated -90^o in orientation relative to the elements in the other diagonal (see Fig. 5b). This sequential feeding mechanism produces two fields with equal magnitude and out of phase by 90^o which results in improving the circular polarization bandwidth of the array.

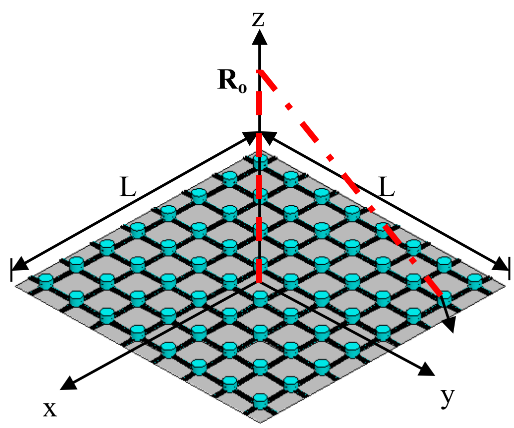

a. 3-D view.

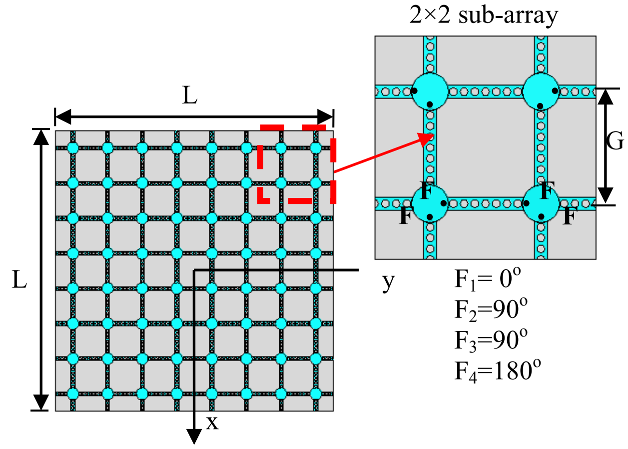

b. Top view

Fig. 5. The geometry of the proposed 8 ×8 RFID reader antenna array consists of 4 sub-array of CDRA with supporting arms.

The antenna array aperture is placed in the (x, y) plane and (x_i, y_i) are the position coordinates of the ith element. The phase of the feeding currents has been adjusted to maximize the radiated field at a distance z = R_o= 40 cm (The assumed boundary for the far field is 2L^2/λ = 306.11 cm) from the antenna aperture. For the NF- focused phased array, the phase shift for the ith element can be calculated from,

$$\phi_i = \frac{2\pi}{\lambda}\left(\sqrt{x_i^2 + y_i^2 + R_o^2} - R_o\right). \tag{2}$$

The beamwidth between 3-dB points in the focal plane is defined as the array spot size. The spot size area radius, W, of a NF-focused planar array depends on the interelement distance, array size and geometry [22]

$$W = 0.8868\, R_o \cdot \frac{\lambda}{L}. \tag{3}$$

In this case, W= 6.52 cm (1.26 λ_o). The Poynting vector is equal to the cross product of electric field, Ē, by the complex conjugate of the magnetic field, Ĥ. The magnitude of its real part is the active power density while the magnitude of its imaginary part is the reactive power density [23].

Adding the phase shift to the array elements results in focusing both the active and reactive power density at the focal plane (the plane includes the focus point). The ratio between the active power density and the reactive power density is very large (about 256). Thus, only the active radiated power density will be taken into account and is given by

$$S = \left\| \mathrm{Re}\left(\vec{S}\right) \right\| = \left\| \mathrm{Re}\left(\vec{E} \times \vec{H}^*\right) \right\|. \tag{4}$$

The equivalent plane wave power density *p* is defined from the E-field or the H-field as follows [21]

$$p = S_e = \frac{\|\vec{E}_x\|^2 + \|\vec{E}_y\|^2 + \|\vec{E}_z\|^2}{\eta_o}, \tag{5}$$

$$or \;\; p = S_h = \eta_o \cdot \left(\|\vec{H}_x\|^2 + \|\vec{H}_y\|^2 + \|\vec{H}_z\|^2 \right)$$

where $\eta_o = 377\Omega$. The normalized power density distribution in the x-y plane for the uniformly phased array compared to that of the NF-focused array is used to introduce the effect of focusing as shown in Fig. 6. The power density of the NF-focused antenna array decreases rapidly from the focal point than that of the uniformly phased array. The -3dB contour curve of the NF-focused array exhibits a diameter of about 8 cm. Contour plots of the normalized power density in the x-z plane is plotted in Fig. 7.

Figure 8 shows the variations of the power density along the z-axis from the antenna aperture of the NF-focused array. The 3-dB focused depth of the array is 31.2 cm along the array axis.

Using a rectangular to spherical coordinate transformation, the three components of the electric field E_x, E_y, and E_z are transformed to their spherical counterpart E_r, E_θ, and E_φ. For NF-focused array, the radial component of the electric field E_r is very small and can be ignored in the near field region [24]. Thus, only the components E_θ and E_φ are used to calculate the axial ratio. The AR in the area of 20 × 20 cm^2 of the transverse plane at focal point 40 cm away from the NF array aperture is shown in Fig. 9. The NF-focused array exhibits focused circular polarization in area around the focal point less than that for the uniformly phased array. The variations of the normalized power density along x-axis and y-axis for the uniformly phased array and NF- focused array are shown Fig. 10. The side lobe level, SLL, in the 32 × 32 cm^2 area around the focal point is less than -13.5 dB while -5.82 dB for the uniformly phased array. Approximately the same field distributions in the far- field region for the uniformly phased array are obtained in the near field region for the NF-focused array due to the phase correction of each element in the array.

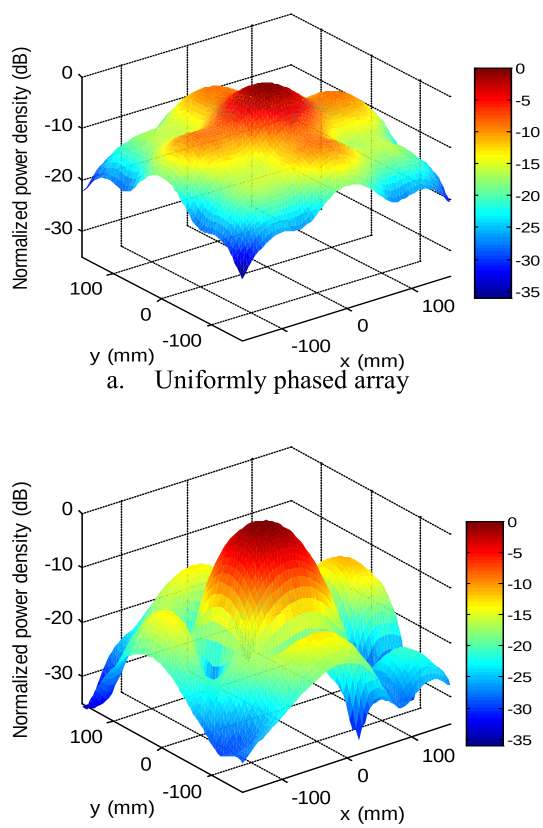

a. Uniformly phased array

b. NF- focused array

Fig. 6. A 3-D plot of the simulated normalized power density of the 8×8 CDRA at z=R_o=40 cm.

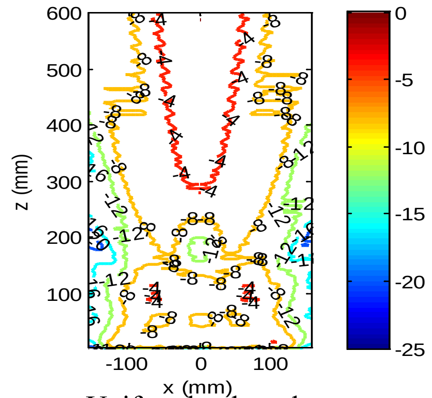

a. Uniformly phased array

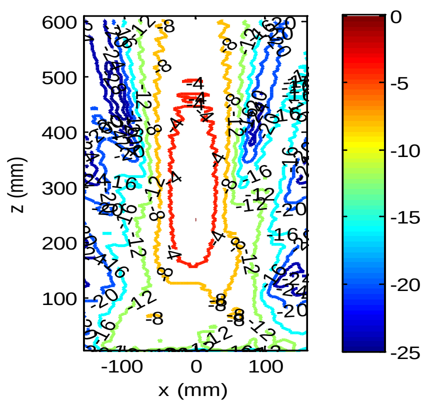

b. NF- focused array

Fig. 7. A contour plot of the simulated normalized power density of the 8×8 CDRA in the x-z plane at y=0.

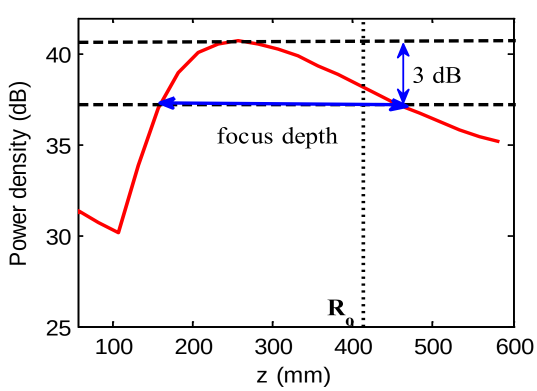

Fig. 8. Simulated radiated power density along the axial direction for the NF-focused CDRA array with supporting arms at x=y=0.

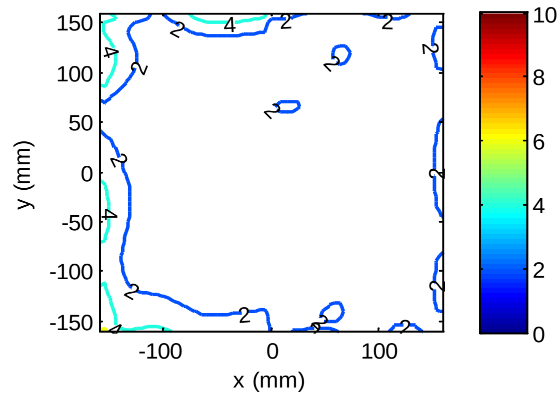

a. Uniformly phased array

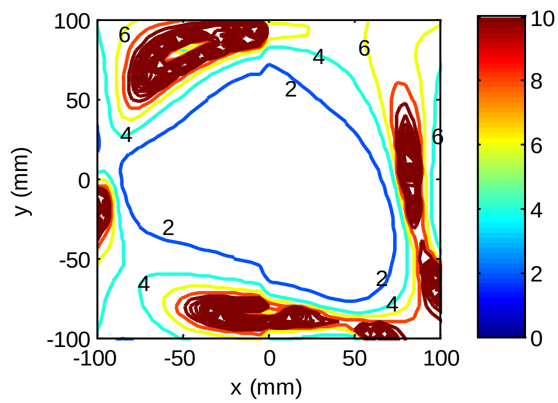

b. NF focused array

Fig. 9. Contour plot of the simulated axial ratio in 20 ×20 cm^2 area at $z=R_o= 40$ cm from the antenna aperture.

IV. CONCLUSION

The performance of the proposed NF- focused CDRA array compared with the uniformly phased CDRA array has been presented. The NF-focused CDRA array is maximizing the radiated power at a limited size spot of radius 6.5 cm in the focal plane at 40 cm from the array aperture with a 3-dB focus depth of 31.2 cm along the axis normal to the array aperture. The NF- focused array produces a far-field like pattern in the near–field at the focal plane. Thus, the near field focused array will improve the performance of the reader antenna for the RFID application, and consequently improve the detectability of the tagged objects in the near field.

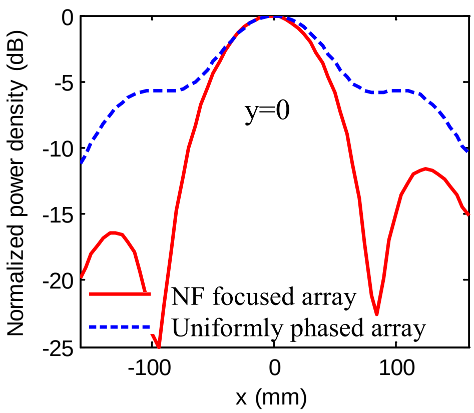

a. x- axis

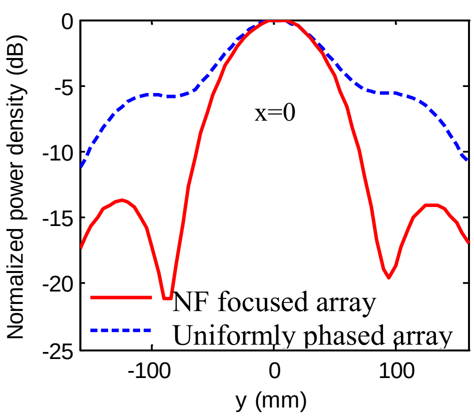

b. y-axis

Fig. 10. Simulated normalized power density along the transverse direction at z=R_o= 40 cm from the antenna aperture.

REFERENCES

[1] K. Finkenzeller, RFID Handbook: Radio-Frequency Identification Fundamentals and Applications, 2nd Ed., *Wiley & Sons, Inc.*, New Jersey, USA, 2004.

[2] R. Bhochhibhoya, Mobile Tag Reading in a Multi-Reader RFID Environment, *M. Sc. Thesis, Pokhara University*, Nepal, India, 2005.

[3] W. Arts, E.D. Mulder, B. Preneel, G.A. Vandenbosch, and I. Verbauwhede, "Dependence of RFID Reader Antenna Design on Read Out Distance," *IEEE Trans. on Antennas and Propag.*, vol. 56, no. 12, pp. 3829-3837, December 2008.

[4] S. H. Zainud-Deen, Hend A. Malhat, and K. H. Awadalla, "Circular Polarized Dielectric Resonator Antenna for Portable RFID Reader using a Single Feed," *International Journal of Radio Frequency Identification & Wireless Sensor Networks*, vol. 1, no.1, 2011.

[5] S. H. Zainud-Deen, H. A. Malhat, and K. H. Awadalla, "Octafilar Helical Antenna for Handheld UHF-RFID Reader," *International Journal of Radio Frequency Identification & Wireless Sensor Networks,* vol. 1, no. 1, 2011.

[6] C. F. Tseng, C. L. Huang, and C. H. Hsu, "A Wideband Planar Inverted-F Dielectric Resonator Antenna for RFID System Applications," *Microwave and Opt. Tech. Letters*, vol. 48, no. 7, pp. 1302-1305, July 2006.

[7] Z. Sun, S. S. Zhong, X. R. Tang, and K. D. Chen, "Low-Side Lobe Circular-Polarized Microstrip Array for 2.45 GHz RFID Readers," *Microwave and Opt. Tech. Letters.*, vol. 50, no. 9, pp. 2235-2237, September 2008.

[8] M. Abbak, and I. Tekin, "RFID Coverage Extension using Microstrip-Patch Antenna Array," *IEEE Antennas and Propag. Magazine,* vol. 51, no. 1, pp. 185-191, February 2009.

[9] M. Bogosanovie and A. G. Williamson, "Microstrip Antenna Array with a Beam Focused in the Near Field Zone for Application in Noncontact Microwave Industrial Inspection," *IEEE Trans. on Instruments and Measurements,* vol. 56, no. 6, pp. 2186-2495, December 2007.

[10] J. T. Loane and S. Lee, "Gain Optimization of Near Field Focusing Array for Hyperthermia Applications," *IEEE Trans. on Microwave Theory and Techniques*, vol. 37, no. 10, pp. 1629-1635, October 1989.

[11] F. R. L. Silva, M. T. de Melo, and M. D. Lourenc¸ O. Junior, "Coplanar Antenna Array Design with Stubs over Dipoles for RFID Applications," *Microwave and Opt. Tech. Letters*, vol. 50, no. 4, pp. 877-879, April 2008.

[12] H. T. Chou, T. M. Hung, N. N. Wang, H. H. Chou, C. Tung, and P. Nepa, "Design of a Near Field Focused Reflectarray Antenna for 2.4 GHz RFID Reader Applications," *IEEE Trans. Antennas Propag.*, vol. 59, no. 3, pp. 1013-1018, March 2011.

[13] H. T. Chou, C. Tung, T. M. Hung, H. H. Chou, and P. Nepa, "Design of a Near Field Focused Reflectarray Antenna for RFID Reader Applications," *in Proc. IEEE Antennas and Propag. Soc. Int. Symp.*, vol. 48, Toronto, Canada, June 2010.

[14] S. H. Zainud-Deen, H. A. Malhat, and K. H. Awadalla, "Near-Field Focused DRA Array for Fixed RFID Reader," *International Journal of Radio Frequency Identification & Wireless Sensor Networks,* vol. 1, no. 1, 2011.

[15] R. Siragusa, P. Lemaître-Auger, and S. Tedjini, "Tuneable Near-Field Focused Circular Phase-Array Antenna for 5.8-GHz RFID Applications,"

IEEE Antennas and Wireless Propag. Letters, vol. 10, pp. 33-36, January 2011

[16] R. Schuhmann, T. Weiland, W. H. Schilders, E. J. Maten, and S. H. Houben, "Recent Advances in Finite Integration Technique for High Frequency Applications," *Scientific Computing in Electrical Engineering,* vol. 4, pp. 46-57, 2004.

[17] J. L. Volakis, A. Chatterjee, and L. C. Kempel, "Finite Element Method for Electromagnetic: Antennas, Microwave Circuits, and Scattering Applications," *IEEE Press*, Piscataway, NJ, 1998.

[18] M.T. Sebastian, Dielectric materials for Wireless Communication, *Elsevier Ltd.*, 2008.

[19] R. Chair, A. A. Kishk, and K. F. Lee, "Experimental Investigation for Wideband Perforated Dielectric Resonator Antenna," *Electronic Letters*, vol. 42, no. 3, pp. 137-139, Feb. 2006

[20] Y. Zhang and A. A. Kishk, "Analysis of Dielectric Resonator Antenna Arrays with Supporting Perforated Rods," *2nd European Conf. on Antennas and Propag., (EuCAP 2007)*, pp. 1-5, 2007.

[21] M. Hansishi and H. Takazawa, "Broad Band Circularly Polarized Planar Array Composed of a Pair of Dielectric Resonator Antennas," *Electronics Letters,* vol. 21, no. 10, pp. 437-438, May 1985.

[22] R. C. Hansen, "Focal Region Characteristics of Focused Array Antennas," *IEEE Trans. Antennas Propag.,* vol. 33, no. 12, pp. 1328-1337, December 1985.

[23] Y. Adanel, M. Wongl, C. Dale', and J. Wiartl, "Near Field Power Density Characterization of Radio Base Station Antennas using Spherical Harmonics Optimization Techniques," *European Conference on Wireless Technology, Amsterdam*, Holland, pp. 121-124, 2004.

[24] A. J. Fenn, "On the Radial Component of the Electric Field for a Monopole Phased Array Antenna Focused in the Near Zone," *IEEE Trans. Antennas Propag.,* vol. 40, no. 6, pp. 723-727, June 1992.

S. H. Zauind-Deen: (S'81-M'88) was born in Menouf, Egypt, on November 15, 1955. He received the B.Sc. and M.Sc. degrees from Menoufia University in 1973 and 1982, respectively, and the Ph.D. degree in Antenna Engineering from Menoufia University, Egypt in 1988.

He is currently a professor in the Department of Electrical and Electronic Engineering in the Faculty of Electronic Engineering, Menoufia University, Egypt. His research interest at present includes microstrip and leaky wave antennas, DRA, RFID, optimization techniques, FDFD and FDTD, scattering problems, and breast cancer detection.

Hend A. Mahat: was born in Menouf, Egypt, on December 12, 1982. She received the B.Sc. and M.Sc. degrees from Menoufia University in 2004 and 2007, respectively, and the Ph.D. degree in Antenna Engineering from Menoufia University, Egypt in 2011.

She is currently a lecturer in the Department of Electrical and Electronic Engineering in the Faculty of Electronic Engineering, Menoufia University, Egypt. Her research interest at present includes Transmitarray, reflectarray, DRA, RFID, and wavelets technique.

K. H. Awadalla: was born in El-Santa – Gharbiya - Egypt, on February 1, 1943. He received the B.Sc. and M.Sc. from Faculty of Engineering, Cairo University, Egypt, in 1694 and 1972, respectively, and the Ph.D. degree from University of Birmingham, UK. in 1978.

He is currently a Professor emeritus in the Dept. of Electrical and Electronic Engineering in the Faculty of Electronic Engineering, Menoufia University, Egypt. His research interest at present includes microtrip and leaky wave antennas, DRA, RFID, and optimization techniques.